J|A|C|S
COMMUNICATIONS

Band Gap Engineering of Quaternary-Alloyed ZnCdSSe Quantum Dots via a Facile Phosphine-Free Colloidal Method

Zhengtao Deng,* Hao Yan, and Yan Liu*

The Biodesign Institute and Department of Chemistry and Biochemistry, Arizona State University, Tempe, Arizona 85287

Received October 2, 2009; E-mail: yan_liu@asu.edu; Zhengtao.Deng@asu.edu

II−VI colloidal semiconductor quantum dots (QDs) such as binary CdSe and CdTe, whose band gaps are continuously tuned by changing their sizes, offer a powerful new tool for use in multicolor bioimaging, biosensing, light-emitting diodes, photovoltaic devices, lasers, and quantum computing devices.[1,2] However, the large size differences between QDs of various colors could cause problems in biomolecule conjugation, superlattice structure formation, and device processing.[3,4] Herein, we initiate a solution to this problem by introducing quaternary-alloyed $Zn_xCd_{1-x}S_ySe_{1-y}$ ($0 \leq x \leq 1$; $0 \leq y \leq 1$) QDs that have uniform size (∼6 nm) but variable compositions that are controlled by tuning the molar ratio of the source materials. The QD band-edge emissions are continuously tunable across the entire visible spectrum (440−650 nm).

Recently, several groups have demonstrated that alloyed QDs have many advantages over binary QDs. For example, Bawendi and co-workers[5] fabricated LEDs using ZnCdSe ternary-alloyed QDs, which enabled easier charge injection than in CdSe/ZnS QDs. Alivisatos and co-workers[6] reported solar cells made of PbS_xSe_{1-x} ternary-alloyed QDs that demonstrated a 2-fold improvement in efficiency over devices composed of either pure PbS or pure PbSe QDs. Very recently, Krauss et al.[7] described "nonblinking" CdZnSe/ZnSe QDs that have an alloyed composition. These findings indicate that alloyed QDs may represent a new route to achieve the next generation of QDs.

Previously, II−VI ternary-alloyed QDs such as CdSeTe, ZnCdSe, ZnCdS, and CdSSe have been synthesized, but the range of tunable band gaps was limited by the QD composition.[3,8] To the best of our knowledge, II−VI quaternary-alloyed QDs with band gaps engineered over the entire visible spectrum have not been achieved to date. Herein, we report the first synthesis of high-quality quaternary-alloyed $Zn_xCd_{1-x}S_ySe_{1-y}$ QDs (ZnCdSSe QQDs) via a facile, "green", phosphine-free, low-cost colloidal method. We demonstrate that the band gap of the ZnCdSSe QQDs can be hybrid-engineered by tuning either the composition or the size. As a result, QQDs that are the same size but have emissions ranging from 440 to 650 nm can be easily synthesized.

The current synthetic technique is modeled on the classic protocol for synthesis of colloidal CdSe QDs, which involves the injection of a tri-*n*-octylphosphine-Se precursor into a Cd precursor solution.[9] Recently, we modified this method by utilizing a "green", phosphine-free solvent for the synthesis of zinc blende CdSe QDs.[10] In the current work, the ZnCdSSe QQDs were obtained by a modified phosphine-free technique of injecting a Zn/Cd precursor into a S/Se precursor in paraffin liquid [see the Supporting Information (SI) for experimental details]. The key to this method is the ability to tune the relative chemical reactivity of the Zn, Cd, S, and Se precursors. For the cation (Zn/Cd) precursors, we discovered that both ZnO and CdO can be well-dissolved in a mixture of oleic acid (OA) and 2-ethylhexanoic acid (EHA). For the anion (S/Se) precursors, we found that direct heating of mixed S/Se powder in paraffin liquid at higher temperature can reduce their chemical reactivity differences.[10] These conditions led to the successful synthesis of our QQDs.

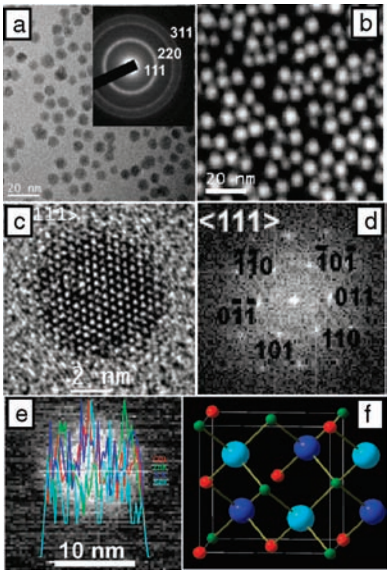

Figure 1. (a) TEM image (inset: indexed SAED pattern) and (b) HAADF-STEM image of typical 6 nm $Zn_{0.6}Cd_{0.4}S_{0.5}Se_{0.5}$ QQDs. (c) HRTEM image and (d) corresponding FFT of a single $Zn_{0.6}Cd_{0.4}S_{0.5}Se_{0.5}$ QQD projected in the ⟨111⟩ direction. (e) STEM-EDS line scan along a single ∼10 nm $Zn_{0.6}Cd_{0.4}S_{0.5}Se_{0.5}$ QQD. (f) Structural model of the QQD lattice projected along the ⟨001⟩ orientation. Structural features: the selenide (cyan) or sulfide (blue) anions occupy half of the tetrahedral holes in the fcc lattice of the cadmium (red) or zinc (green) cations.

Transmission electron microscopy (TEM) and high-angle annular dark-field scanning transmission electron microscopy (HAADF-STEM) images (Figure 1a,b and Figure S1 in the SI) show that the typical $Zn_{0.6}Cd_{0.4}S_{0.5}Se_{0.5}$ QQD sample was virtually monodispersed. The selected-area electron diffraction (SAED) pattern of the ZnCdSSe QQDs could be indexed to a single face-centered-cubic (fcc) phase. Duplicate phases were not observed, indicating that the sample was uniformly alloyed. Figure 1c,d and Figure S2 in the SI show high-resolution TEM (HRTEM) images and the corresponding indexed fast Fourier transforms (FFTs) of a single QQD projected in the ⟨111⟩, ⟨110⟩, ⟨100⟩, and ⟨211⟩ directions, respectively. The well-resolved lattice images indicate a uniform particle with a highly ordered crystalline structure and a continuously resolved lattice and show no indication of any core−shell structure. Moreover, as shown in Figure 1e, a STEM−EDS line scan through the center of a single ∼10 nm $Zn_{0.6}Cd_{0.4}S_{0.5}Se_{0.5}$ QQD revealed the presence of Zn, Cd, S, and Se spanning the entire width of the particle, with no element confined to a narrow region and no core−shell or smaller domains observed. This indicates that

10.1021/ja908408m

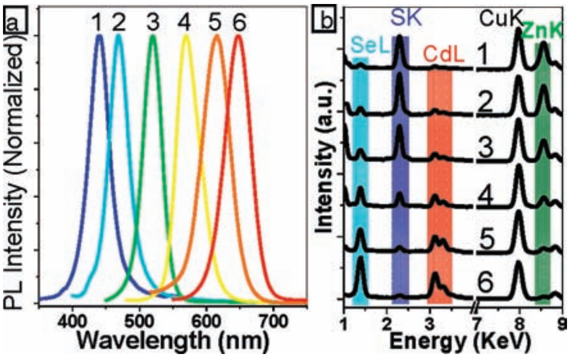

Figure 2. Composition-dependent band-edge emission of ZnCdSSe QQDs. (a) PL emission and (b) TEM−EDS spectra of a series of ~6 nm QQD samples with varying composition. The compositions (x, y) as determined by TEM−EDS are: 1 (0.90, 0.89), 2 (0.80, 0.71), 3 (0.69, 0.59), 4 (0.41, 0.40), 5 (0.25, 0.24). and 6 (0.11, 0.10).

ZnCdSSe QQDs are a uniform alloy of the four elements Zn, Cd, S, and Se, as demonstrated in the structure model shown in Figure 1f.

Figure 2 demonstrates that the band gaps of the ZnCdSSe QQDs can be continuously tuned across the entire visible spectrum by adjusting the relative amounts of the four elements. This can be easily accomplished by varying the molar ratios of the source materials. Figure 2a shows photoluminescence (PL) data for a series of ZnCdSSe QQDs with band-edge emission peaks at 440, 470, 515, 570, 615, and 650 nm, respectively. The red shift of the PL emission peaks as the QQD composition goes from ZnS-rich to CdSe-rich is due to the narrower band gap of CdSe than of ZnS. Elemental analysis of ensembles of QDs using TEM-based energy-dispersive X-ray analysis (TEM−EDS) (Figure 2b) revealed the presence of Zn, Cd, S, and Se with compositions identified as $Zn_{0.90}Cd_{0.10}S_{0.89}Se_{0.11}$, $Zn_{0.80}Cd_{0.20}S_{0.71}Se_{0.29}$, $Zn_{0.69}Cd_{0.31}S_{0.59}Se_{0.41}$, $Zn_{0.41}Cd_{0.59}S_{0.40}Se_{0.6}$, $Zn_{0.25}Cd_{0.75}S_{0.24}Se_{0.76}$, and $Zn_{0.11}Cd_{0.89}S_{0.10}Se_{0.90}$. Low-magnification TEM images (Figure S3 in the SI) indicated that all of the various QQDs had the same diameter of ~6 nm and a narrow size dispersion (σ) of 5−10%. Powder X-ray diffraction (XRD) patterns of the samples (Figure S4 in the SI) showed that all the ZnCdSSe QQDs can be indexed to a single face-centered cubic (fcc) phase. The diffraction peaks shifted gradually toward smaller angles in going from sample 1 to 6, indicating increasing lattice constants of the QDs with gradual substitution of Zn and S atoms with the bigger and heavier Cd and Se atoms, in accord with Vegard's law.[10] We measured the PL quantum yield of the QQDs with a cross-calibrated protocol (see the SI). The PL quantum yields were found to be between 40 and 65%. These results clearly demonstrate that our ZnCdSSe QQDs have uniform size, high PL quantum yields, and composition-dependent emission peaks tunable from 440 to 650 nm. Such properties may be beneficial for applications requiring uniformly sized QDs with varying optical properties.

To further demonstrate the high programmability of our QQD system, we engineered the band gaps of the ZnCdSSe QQDs by tuning the particle size while maintaining the same composition [i.e., (x, y)]. Four different sizes of QQDs with diameters of ~4, ~5, ~7, and ~10 nm (σ from 5 to 12%) and corresponding emission peaks at 528, 555, 575, and 600 nm are shown in Figure 3. The blue shift of the PL emission peaks with decreasing QD size is due to the quantum-confinement effect. TEM−EDS analysis (Figure S6 in the SI) revealed the presence of Zn, Cd, S, and Se in all four samples. Quantitative analysis showed that their compositions were nearly the same as $Zn_{0.6}Cd_{0.4}S_{0.5}Se_{0.5}$. This also indicates that the QD samples are uniformly alloyed without any significant composition change occurring throughout the entire growth process.

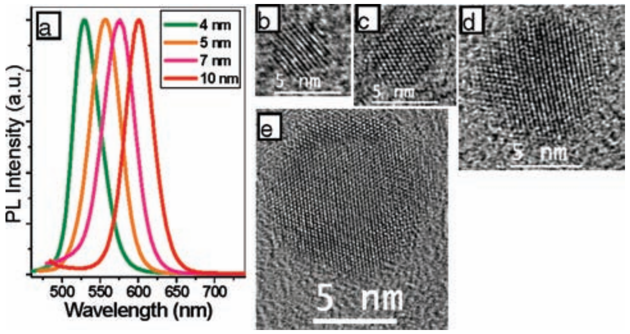

Figure 3. Size-dependent band-edge emission of ZnCdSSe QQDs. (a) PL emission spectra and (b−e) HRTEM images of a series of $Zn_{0.6}Cd_{0.4}S_{0.5}Se_{0.5}$ QQD samples with varying size.

In summary, we have reported the first synthesis of high-quality quaternary-alloyed $Zn_xCd_{1-x}S_ySe_{1-y}$ colloidal QDs across the entire compositional range (x, y) = 0 to 1. The band gap of the new QDs could be hybrid-engineered by tuning either the QD composition or size. Such QQDs are easy to synthesize and have high photoluminescence quantum yields without the necessity of overcoating a shell. We believe that these QQDs could find broad use in multicolor bioimaging, biosensing, light-emitting diodes, solar cells, and other nanodevice applications.

Acknowledgment. We thank ONR, ARO, NSF, and NIH for financial support of Y.L. and ONR, NSF, NIH, ARO, AFOSR, DOE, and a Sloan Research Fellowship for financial support of H.Y.

Supporting Information Available: Additional synthesis and characterization details. This material is available free of charge via the Internet at http://pubs.acs.org.

References

(1) Bruchez, M.; Morrone, P.; Gin, S.; Weiss, S.; Alivisatos, A. P. *Science* **1998**, *281*, 2013. Chan, W. C.; Nie, S. *Science* **1998**, *281*, 2016. Qi, L. F.; Gao, X. H. *ACS Nano* **2008**, *2*, 1403. Smith, A. M.; Nie, S. *Nat. Biotechnol.* **2009**, *27*, 732. Zrazhevskiya, P.; Gao, X. H. *Nano Today* **2009**, *4*, 414.
(2) Klimov, V. I.; Mikhailovsky, A. A.; Xu, S.; Malko, A.; Hollingsworth, J. A.; Leatherdale, C. A.; Eisler, H. J.; Bawendi, M. G. *Science* **2000**, *290*, 314. Sun, Q.; Wang, Y. A.; Li, L. S.; Wang, D. Y.; Zhu, T.; Xu, J.; Yang, C. H.; Li, Y. F. *Nat. Photonics* **2007**, *1*, 717.
(3) Bailey, R. E.; Nie, S. M. *J. Am. Chem. Soc.* **2003**, *125*, 7100.
(4) Anikeeva, P. O.; Halpert, J. E.; Bawendi, M. G.; Bulovic, V. *Nano Lett.* **2009**, *9*, 2532.
(5) Caruge, J. M.; Halpert, J. E.; Wood, V.; Bulovic, V.; Bawendi, M. G. *Nat. Photonics* **2008**, *2*, 247.
(6) Ma, W.; Luther, J. M.; Zheng, H.; Wu, Y.; Alivisatos, A. P. *Nano Lett.* **2009**, *9*, 2072.
(7) Wang, X.; Ren, X.; Kahen, K.; Hahn, M. A.; Rajeswaran, M.; Maccagnano-Zacher, S.; Silcox, J.; Cragg, G. E.; Efros, A. L.; Krauss, T. D. *Nature* **2009**, *459*, 686.
(8) Zhong, X.; Han, M.; Dong, Z.; White, T. J.; Knoll, W. *J. Am. Chem. Soc.* **2003**, *125*, 8589. Zhong, X.; Feng, Y.; Knoll, W.; Han, M. *J. Am. Chem. Soc.* **2003**, *125*, 13559. Swafford, L. A.; Weigand, L. A.; Bowers, M. J., II; McBride, J. R.; Rapaport, J. L.; Watt, T. L.; Dixit, S. K.; Feldman, L. C.; Rosenthal, S. J. *J. Am. Chem. Soc.* **2006**, *128*, 12299.
(9) Murray, C. B.; Norris, D. J.; Bawendi, M. G. *J. Am. Chem. Soc.* **1993**, *115*, 8706. Peng, Z. A.; Peng, X. *J. Am. Chem. Soc.* **2001**, *123*, 183.
(10) Deng, Z.; Cao, L.; Tang, F.; Zou, B. *J. Phys. Chem. B* **2005**, *109*, 16671. Deng, Z. T.; Mansuripur, M.; Muscat, A. J. *Nano Lett.* **2009**, *9*, 2015.

JA908408M